Nat Hazards
DOI 10.1007/s11069-011-9840-6

ORIGINAL PAPER

Displacement patterns of a landslide affected by human activities: insights from ground-based InSAR monitoring

Francesca Bozzano · Ivan Cipriani · Paolo Mazzanti · Alberto Prestininzi

Received: 8 September 2010 / Accepted: 28 April 2011

Abstract Landslides interacting with large infrastructures represent a major problem for the economy, society as a whole, and the safety of workers. Continuous monitoring for 23 months using an integrated platform with a ground-based SAR interferometer (GB-InSAR), a weather station, and an automatic camera gave us the opportunity to analyze the response of an unstable slope to the different phases of work. The deformational behavior of both the natural slope and the man-made structures was recorded and interpreted in relation to the working stages and the rainfall conditions during the whole monitoring period. A typical pattern of displacement was identified for shallow landslides, debris produced by the excavation and gabions, metallic walls, and anchored bulkheads. Furthermore, insights into the dynamics and behavior of the slope and the man-made structures that interact with the landslide were obtained. Extreme rainfall is the main trigger of shallow landslides and gabion deformations, while anchored bulkheads are less influenced by rainfalls. Movement of debris that is produced by excavations and temporary metallic barrier deformation are closely related to each other. The herein proposed monitoring platform is very efficient in monitoring unstable slopes that are affected by human activities. Moreover, the recorded patterns of displacement in the slope and the man-made structures can be used as reference data for similar studies and engineering designs.

Keywords GB-InSAR · Interferometry · Landslide · Monitoring · Displacement · Infrastructure

F. Bozzano · P. Mazzanti · A. Prestininzi
CERI, Research Centre on Prevention, Prediction and Control of Geological Risks, P.zza U. Pilozzi 9, 00038 Valmontone, Italy

F. Bozzano · I. Cipriani · P. Mazzanti (✉) · A. Prestininzi
Dipartimento di Scienze della Terra, "Sapienza" Università di Roma, P.le Aldo Moro 5, 00185 Rome, Italy
e-mail: paolo.mazzanti@uniroma1.it

F. Bozzano · P. Mazzanti
NHAZCA S.r.l., Spin-Off "Sapienza" Università di Roma, Via Cori snc, 00177 Rome, Italy

Published online: 27 May 2011

1 Introduction

Landslides represent a major threat for mankind. They are natural phenomena controlled by gravity and sometimes triggered by external natural factors (rainfalls, earthquakes, volcanic eruptions, etc.) as well as by human landscape modifications. Constant population growth and increasing mobility intensify the alteration of the landscape. Human settlements, communication roads, and major infrastructures that are constructed in sloping regions, or at the base of mountains, severely expose mankind to landslides. Several catastrophic landslides over the last 100 years have been caused by human carelessness (see at Muller 1968; Sammarco 2004; Guadagno et al. 1999; among the others) when modifying the landscape. However, if suitable monitoring systems are implemented, landslides can be controlled and, in some cases, predicted.

In recent years, greater efforts by the scientific community have led to a deepening knowledge of these phenomena. Furthermore, several innovative instruments are now available to monitor the activity of slopes that interact with human settlements and infrastructure. Among these, a particular interest has been recently devoted to remote sensing apparatus that are based on terrestrial, aerial, or satellite platforms. Remote sensing instruments are characterized by the following advantages with respect to on-site instruments: (a) simultaneous investigation of large areas; (b) safe operability (especially for sensors that do not require on-site targets); and (c) limited interaction with the landslide. Nevertheless, some limitations must be accounted for when remote sensing instruments are used, such as the capability to detect only surface features (e.g., displacement).

The most common remote sensing techniques for landslide monitoring are as follows: (1) photogrammetry (Kraus et al. 1997); (2) laser distance meters and total stations; (3) laser scanner (Teza et al. 2007); (4) radar interferometry (Massonet and Fiegl 1998); and (5) Global Positioning Systems (Brunner et al. 2003). The increasing number of scientific papers dealing with unstable slopes, which are continuously monitored by remote sensing instruments (e.g., Blikra and Anda 2006; Pugliesi et al. 2004), indicates that these techniques are becoming a fundamental tool for the control and mitigation of landslide risk.

In this paper, the results of continuous ground-based SAR interferometric monitoring of a slope affected by human activities are presented. An integrated monitoring platform—consisting of one GB-InSAR instrument, a weather station, and a digital camera—was installed in front of a slope, and it continuously collected data during the different phases of work. Hence, several patterns of displacement, both in the slope and in the man-made structures, were observed and interpreted, shedding light on the overall dynamics of the slope and permitting to work in safe conditions.

2 The study area

The case study described in this paper is particularly complex in terms of both the project's strategic importance and site-specific issues. It concerns a section of a major road imperatively planned on an unstable slope that is characterized by very complex geological and geomorphological features. Few years ago, during some preliminary working activities, a shallow translational landslide (with a volume of about 10^4 m^3) affected the slope, thus completely destroying the already constructed structures.

Following this event, detailed geological-engineering investigations and surveys (field geomorphological, geological, and geomechanical surveys, boreholes, seismic surveys, and

laboratory tests of samples) were carried out. Hence, a geological model able to explain the occurrence of this landslide was built (Fig. 1).

The steep relief consists of jointed and weathered metamorphic rocks. A Pliocene and Pleistocene sandy marine deposit overlies most of the elevated portion of these rocks, while sandy colluvial deposits a few meters thick constitute an irregular blanket along the slope. Furthermore, geological and geomorphological evidence of an old deep rotational slide that involved a total volume of about 1×10^6 m^3 was identified in the slope where intensively jointed gneiss and Pliocene and Pleistocene sands outcrop. The main sliding surface (up to 50 m deep) and some secondary surfaces were reconstructed from a geomorphological survey and stratigraphic logs. Minor shallow translational landslides have been surveyed in the middle-lower part of the preexisting largest landslide. They involve volumes of about 1×10^4 m^3 of colluvial deposits and bedrock. Among these, we can include the landslide that destroyed the already-built structures.

From the climatic point of view, the study area is characterized by a Mediterranean climate (Pinna 1972). The pluviometric regime is characterized by intense rainfalls in autumn, winter, and spring, with less intense events during the summer. The annual average precipitation in this area is about 1,148 mm, and the upper values historically registered are close to 2,300 mm/year. The maximum daily intensity historically reported is about 120 mm (Capra et al. 2004).

The above-described geological model was used as a conceptual basis to design the stabilization works. According to this model, the reactivation of both the whole old landslide and the part of it is plausible because of slope reprofiling and excavation activities. Therefore, some stabilization works were performed, and a continuous monitoring system was used in order to (1) monitor the evolution of the slope under undisturbed

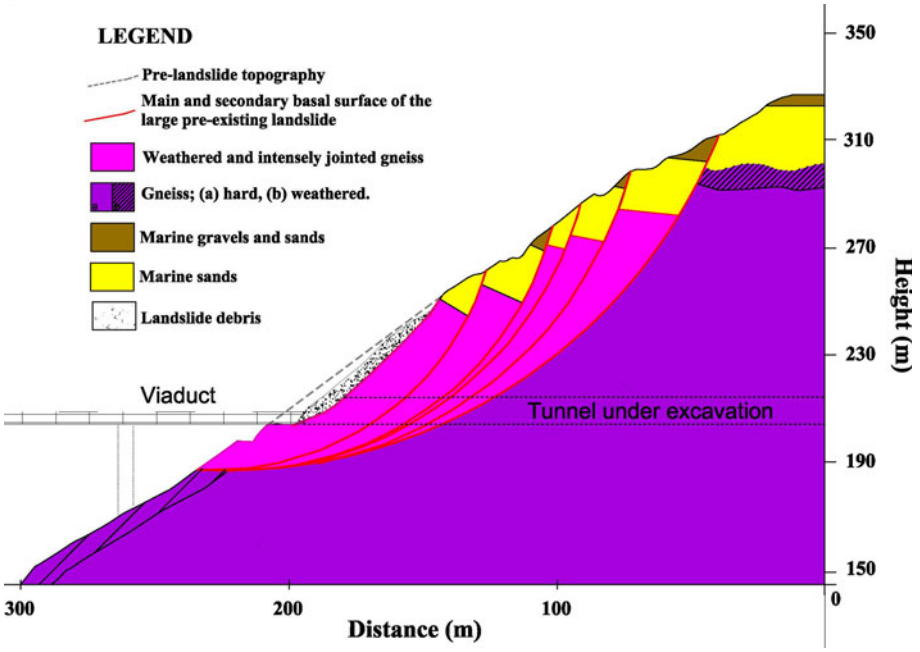

Fig. 1 Geological cross-section of the monitored slope

conditions and during construction, and (2) predict the occurrence of critical conditions, if any. This system would also optimize planning, design, and construction activities and protect the construction site personnel.

3 The slope monitoring

In the frame of this study, an integrated platform made up of a ground-based SAR interferometer model IBIS-L (by IDS S.p.A.), an automatic digital camera, and a wireless weather station was built (Bozzano et al. 2008).

The system was housed in a specially designed box and installed on a slope in front of that one involved in the project, at a distance ranging from 700 to 900 m (Fig. 2).

The digital camera and the weather station, which both have an automatic data acquisition system and transfer data to the controlling PC, play a key role in monitoring activity. The images, which are constantly supplied by the camera, make it possible to continuously monitor the construction activities on the investigated slope, thereby optimizing data collection and processing; this feature also facilitates the interpretation of the results.

The monitoring platform was continuously active from November 2007 to September 2009 (period that the present paper refers to) and collected more than 14,000 photos, 170,000 measurements of weather data, and 160,000 SAR maps (whose features are reported in Table 1).

3.1 Basic principles of GB-InSAR technique

Synthetic aperture radar interferometry (InSAR) is a powerful technique for monitoring of displacement. This technique, which can be applied by satellite, aerial, or terrestrial sensors, is based on the SAR principle (Curlander and McDonough 1991) and the interferometric approach (Hanssen 2001). Ground-based SAR maps, achieved by the combination

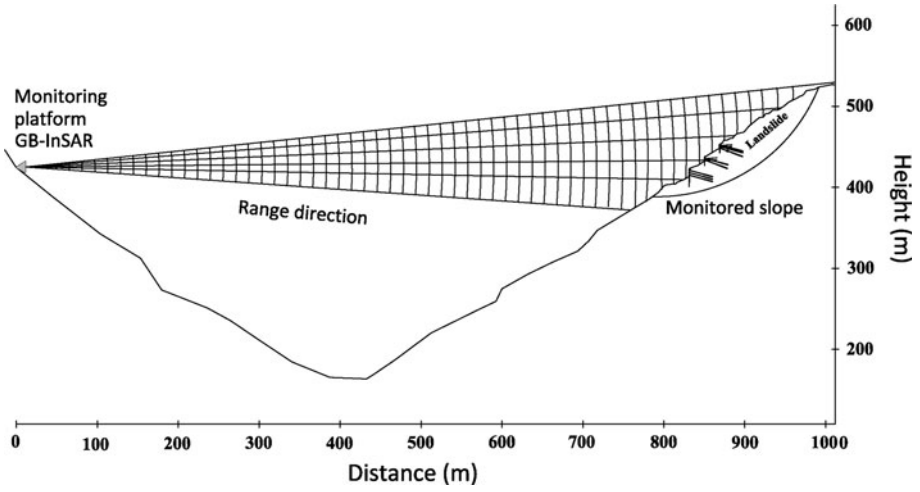

Fig. 2 Sketch showing the monitoring geometry

Table 1 Instrumental configuration of the GB-InSAR interferometer

Rail length	2 m
Central frequency	16.75 GHz
Bandwidth	300 MHz
Polarization	VV
Antenna gain	20 dB
Number of scans in the SAR image	401
Range resolution	0.50 m
Cross-range resolution (3.6 m at a distance of 800 m)	4.5 mrad
Max distance	1,200 m
Inter-scan delay (waiting time between the end of one scan and the start of the next scan)	6 s
Measurement time interval	~6 min

of several radar images collected while the antennas move along a rail, consist of 2D images having a high range and cross-range ("azimuth") resolution (Curlander and McDonough 1991) (Fig. 3). Hence, the final SAR image consists of several pixels, the size of which strongly depends on the equipment, the radar to scenario distance and the acquisition parameters.

By computing the phase difference between all the pixels of at least two SAR maps, collected at different times, a displacement map can be obtained (Hanssen 2001; Antonello et al. 2004).

The atmospheric contribution to the phase difference (which adds to the real slope displacements) may be removed via different postprocessing techniques (Iannini et al. 2009; Noferini et al. 2005; Pipia et al. 2006). The simplest one is based on a GCP (ground control point) technique; by this technique, atmospheric displacements are removed by considering stable reference points within the scenario.

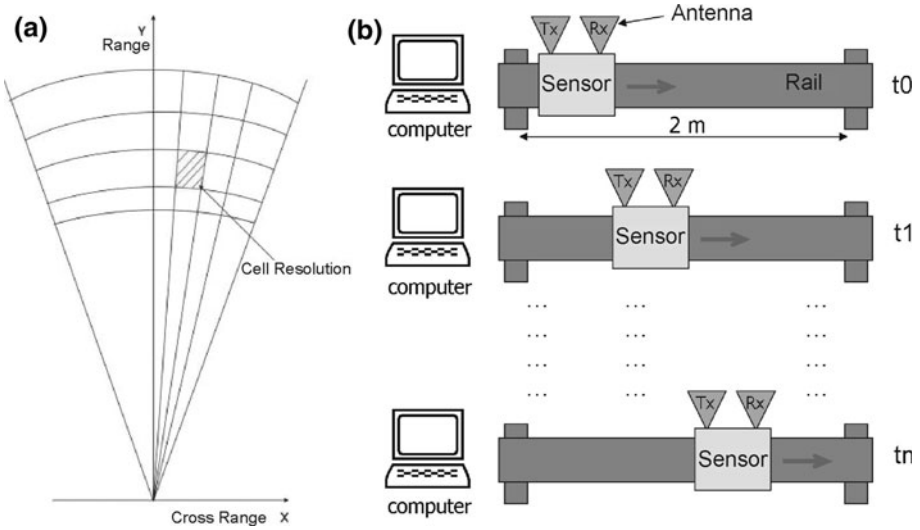

Fig. 3 **a** SAR image acquisition grid; **b** schematic diagram of the ground-based SAR interferometer operation principle

It must be noted that by this technique, only the component of the displacement vector along the line of sight (LoS) can be assessed. The LoS vector represents the line joining the radar to each point of the observed scenario; thus, each pixel of the radar image has a different LoS.

Negative displacement values indicate a movement toward the sensor (shortening along the LoS), while positive displacement values indicate a movement away from the sensor (lengthening along the LoS).

In recent years, GB-InSAR demonstrated its high potential for monitoring volcanic deformations (Casagli et al. 2009), snow cover (Martinez-Vazquez and Fortuny-Guash 2006), and, above all, landslides (Antonello et al. 2004; Barla et al. 2010; Bozzano et al. 2010; Casagli et al. 2010; Corsini et al. 2006; Mazzanti and Brunetti 2010; Noferini et al. 2007; Pieraccini et al. 2002; Tarchi et al. 2003). It has been demonstrated that the following features make GB-InSAR technique particularly suitable for monitoring of landslides that occur in a small area and that are characterized by a fast evolution:

1. high SAR image sampling frequency (few minutes);
2. operation under any weather and lighting condition;
3. complete remote operability, because it does not require the installation of target sensors on the monitored slope;
4. accuracy in the displacement measurement ranging from few tens of millimeters to few millimeters;
5. continuous areal monitoring of the whole slope with a high pixel resolution (from half to a few meters based on the distance);
6. long-range operability (up to 4 km).

4 Data analysis and interpretation

In this paper, the results of 23-month monitoring are reported and interpreted by taking into consideration the different portions of the slope during the excavation and construction phases (Fig. 4).

The following five patterns of displacement were recorded in different portions of the slope also in relation to different construction phases:

- shallow landslides;
- excavated debris;
- retaining walls;
- gabions;
- anchored bulkhead.

In what follows, these patterns will be described in terms of the maximum displacement, velocity, acceleration, and duration in relation to the construction activities and rainfalls. Possible causes and triggering factors for these patterns of displacement will be discussed.

4.1 Shallow landslides

Displacements of small-sized shallow landslides (characterized by volume ranging from 10^1 to 10^3 m^3) were recorded several times and in different parts of the slope during the monitoring activities. These events, that mobilized colluvial material and intensely jointed

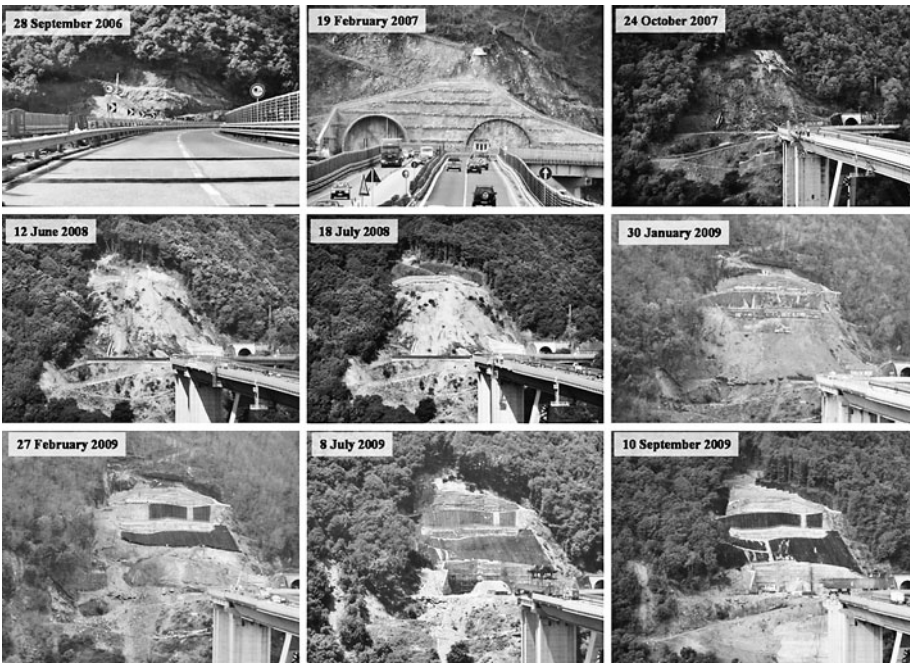

Fig. 4 Pictures showing the overall slope and its main changes from September 2006 to September 2009

bedrock, sometimes caused failures and collapses. Three main areas affected by these events were detected (Fig. 5).

Area α (Fig. 5) was a perched remnant mass of the above-mentioned translational landslide that destroyed man-made structures some years ago. This mass occupied a volume of about 1,000 m^3; it was constituted by gneiss blocks that were immersed in a sandy matrix. This part of the slope moved from the beginning of the monitoring (November 2007) until April 2008, when the unstable mass was completely removed by excavation. The total amount of displacement was on the order of 350 mm. The velocity of the LoS displacement spanned between 50 and 2 mm/day and showed the maximum peak immediately after the March 28, 2008 rainfall (144 mm/day). Figure 6 shows the cumulative displacement map during the period of November 10, 2007 to February 29, 2008. Figure 7 shows the time series of displacement and rainfall in the same period. Trenches that were located immediately above this area represented the clearest effects of the displacement on the slope. However, this part of the slope did not collapsed before it was removed by excavations.

Area β (Fig. 5) is characterized by the outcropping of colluvial material. It was active since the beginning of monitoring and showed a total displacement on the order of 100 mm. In this area, a retaining concrete wall was present until December 2007; then, the wall collapsed due to back-slope failure induced by intense rainfall. Nevertheless, the displacement also continued after the collapse of the wall. In Fig. 8, 10-day-long time series of the displacements and rainfall are presented. Displacement occurred during an intense rainfall, exceeding 100 mm/day.

Area γ (Fig. 5) was never affected by construction and excavation activities because it is located to the side of the yard. In this area, where intensely jointed and weathered gneiss

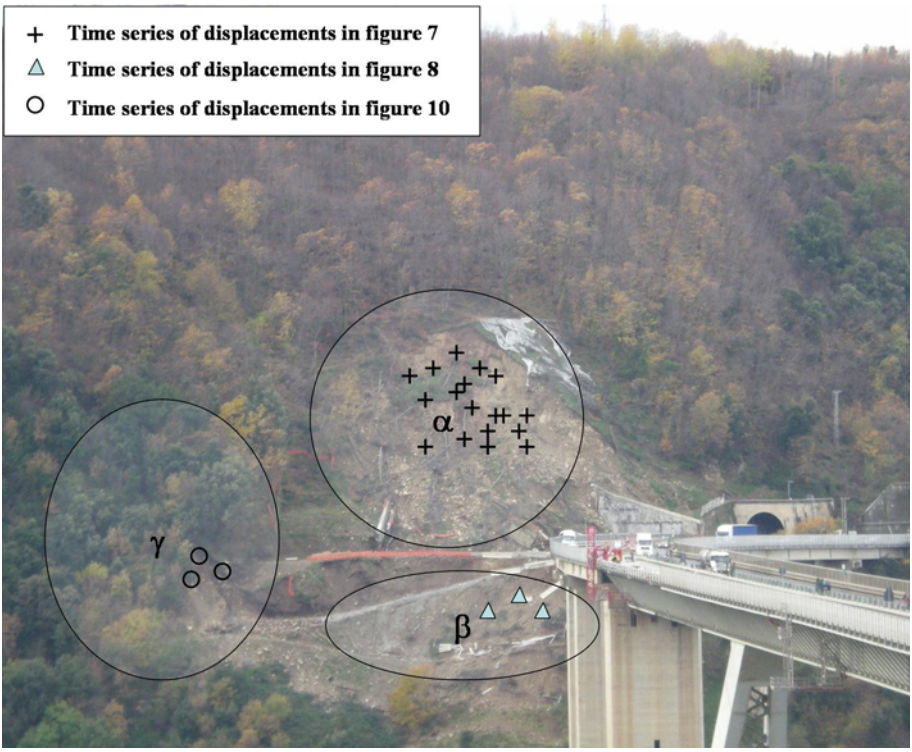

Fig. 5 Picture of the slope and identification of the three areas with homogeneous behavior described in the text and related pixels of Figs. 7, 8, and 10 (areas of interest are included in the black ellipses)

rocks and colluvial material widely outcrop, multistage rock slides and rock falls occurred since the beginning of the monitoring (Fig. 9). These phenomena widened the exposed slope, which was previously covered by trees and, hence, not visible by the monitoring platform.

Displacements in this area have been detected since January 15, 2009 until September 2009. Figure 10a shows time series of the displacements and rainfall of some points located in this area from January 15, 2009 to February 21, 2009.

In what follows, we mainly focus on the slide that occurred on January 24, 2009, which was monitored in detail by GB-InSAR during its whole evolution. Figure 10b shows the time series of the displacement and the rainfall a few days before the collapse. The slope deformation had started about 3 days before the slope collapsed and maintained a rate of displacement of 1–2 mm/day until 24 h before the failure. Then, the slope experienced a rapid increase in the rate of displacement that reached a maximum value of about 12 mm/h (Fig. 10c). At around 3 p.m. on January 24, the slope failed after it had reached a total displacement ranging from 100 to 200 mm. The maximum prefailure displacement (200 mm) was recorded in the upper part of the slope, which was close to the landslide's scar, while the smallest one (100 mm) was recorded in its lower part. Furthermore, while the lower part stopped moving immediately after failure, the upper part was continuing to move, thus reaching a total displacement of about 900 mm after 1 month. Preliminary back-analyses that are based on the inverse velocity method proposed by Fukuzono (1985) allowed to predict the time of slope's failure very accurately (Fig. 10c).

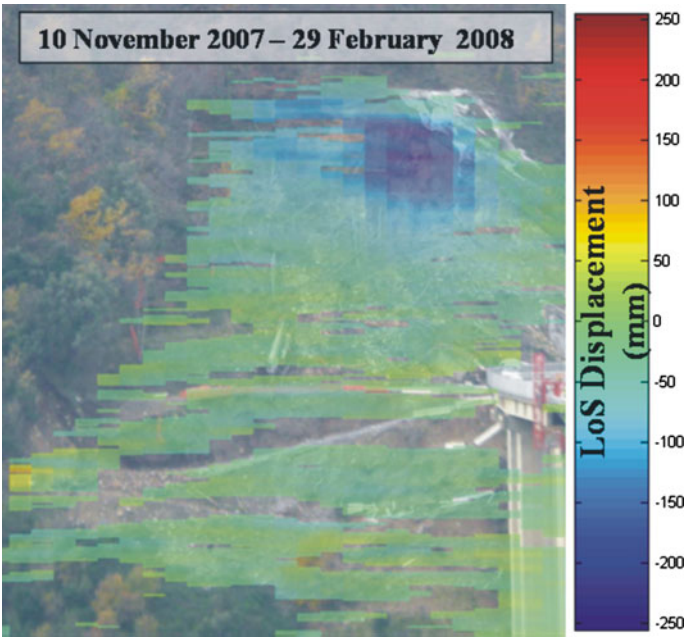

Fig. 6 Picture of the slope that is overlaid by the GB-InSAR LoS displacement map from November 10, 2007 to February 29, 2008

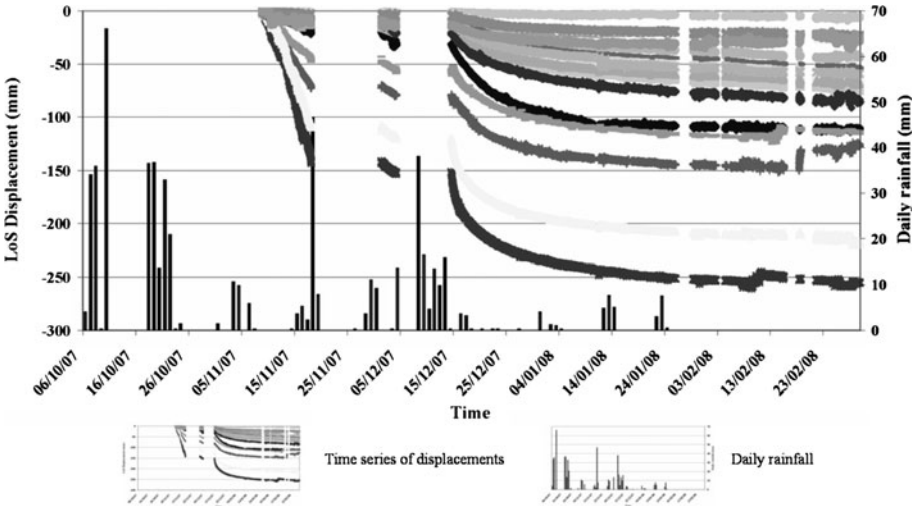

Fig. 7 Daily rainfall and the time series (October 6, 2007 to February 29, 2008) of displacement of some pixels located in area α

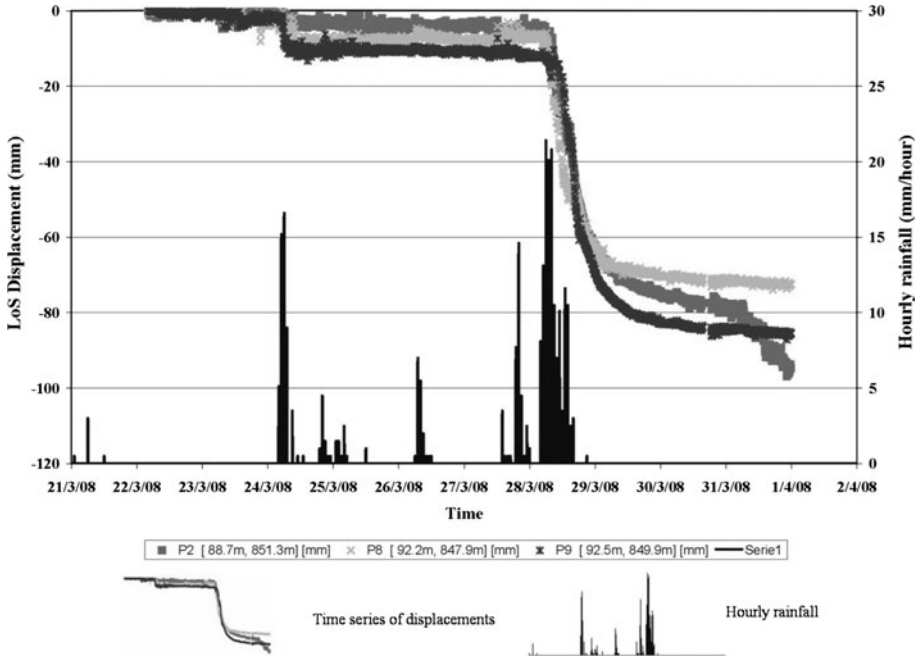

Fig. 8 Hourly rainfall and time series of the displacement of some pixels located in area β (March 22, 2008 to March 31, 2008)

4.2 Debris produced by excavations

On April 2008, excavations started on the slope; as a consequence, a large amount of mobilized debris that was made of sand and colluvial material was produced. This material settled on the lower part of the slope, which had a slope angle of about 30°–40° (Fig. 1). Since its deposition, this material started to move. The movement showed significant acceleration during rainfalls (Figs. 11, 12) and concomitantly (or immediately after) the excavation phases, during which this debris was deposited.

A total LoS displacement of about 5,600 mm was recorded from the beginning of the excavation (April 2008) until the end of January 2009, with a maximum velocity of about 200 mm/day. Figure 12 also shows the quite instantaneous response of the surface debris movement to rainfall. Figure 13 shows the map of total displacement recorded between July 1, 2008 and January 31, 2009. The displacement is quite regular in the entire area with a small decreasing gradient moving to the side of the area covered by debris, which is probably due to the smaller thickness of debris. A qualitative field confirmation of this displacement is provided by rapid changes in the slope's morphology, by the movement of the blocks inside the debris and by the effects induced in the retaining walls, which were originally located in the lower part of the slope (Prg. 4.3).

4.3 Retaining walls

Between December 2007 and March 2008, a metallic wall (Figs. 4, 11), founded on short piles, was built downslope the debris in order to protect the track from the upcoming debris produced by the excavation. The wall did not show any displacement from its installation

Fig. 9 Pictures sequence showing the evolution of the γ area from January 24, 2009 to February 17, 2009

until August 2008. Then, it started to move in September 2008 when debris coming from the upper slope started to push on it (Fig. 11).

The wall was affected by a limited but regular displacement from August 2008 to the end of January 2009, thus reaching a maximum velocity that was on the order of 5.5 mm/day. In this phase, it only showed small displacement accelerations related to significant increases in the displacement rate of the upcoming debris (Fig. 14).

On January 27, 2009, the wall failed. This was the last event of a continuous period of displacement, and it was interpreted as the result of increasing loads that were exerted by the upcoming debris on the back of the wall.

A further effect of the movement of the debris was the progressive overturning of a large remaining portion of a concrete wall destroyed by a landslide that had occurred some years ago and that was encompassed by debris. Movement that decreased from the upper to the lower part of the concrete wall was observed, which is consistent with a movement induced by the sliding of the surrounding debris.

4.4 Gabions

Construction of the gabions (suitable for the protection of man-made cuts) began in May 2008 in the upper part of the slope. Gabions are cages filled with gravel and large blocks; they are very deformable structures and are extensively used in civil and geotechnical engineering.

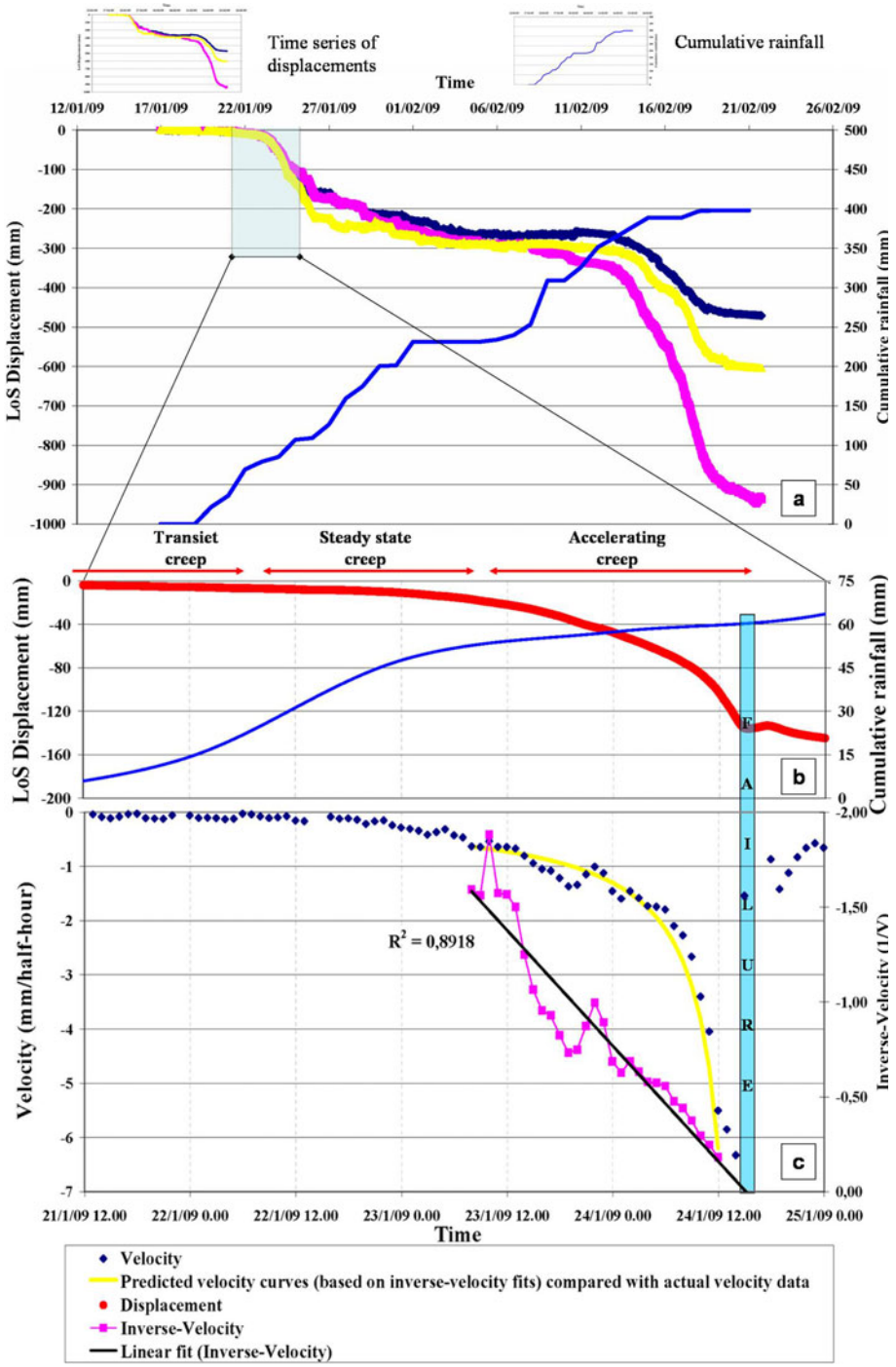
Time series of displacements
Cumulative rainfall
Time
12/01/09
17/01/09
22/01/09
27/01/09
01/02/09
06/02/09
11/02/09
16/02/09
21/02/09
26/02/09
LoS Displacement (mm)
Cumulative rainfall (mm)
a
Transiet creep
Steady state creep
Accelerating creep
b
FAILURE
c
R^2 = 0,8918
Velocity (mm/half-hour)
Inverse-Velocity (1/V)
21/1/09 12.00
22/1/09 0.00
22/1/09 12.00
23/1/09 0.00
23/1/09 12.00
24/1/09 0.00
24/1/09 12.00
25/1/09 0.00
Time
Velocity
Predicted velocity curves (based on inverse-velocity fits) compared with actual velocity data
Displacement
Inverse-Velocity
Linear fit (Inverse-Velocity)

◀**Fig. 10** **a** Cumulative rainfall and displacement time series of some pixels that are located in area γ from January 17, 2009 to February 21, 2009. **b** Time series (January 21, 2009 to January 24, 2009) of the displacement of one pixel that is located in area γ and cumulative rainfall. **c** Time series (January 21, 2009 to January 24, 2009) of the velocity and the inverse velocity of one pixel that is located in area γ. The linear fit of 1/v versus time identifies the time of failure (following Fukuzono, 1985)

Since their construction, these structures showed a peculiar behavior with a generally motionless condition that was sometimes interrupted by short (up to 2–3 days) displacement events.

The first displacement event was recorded on June 3, 2008 (i.e., few days after the construction of the gabions), when a limited portion of the gabion was affected by a displacement up to 50 mm in a very short time interval (a few hours), reaching velocities up to 15 mm/h. No external triggering factors, such as rainfall or construction activity, were recorded; thus, only gravitational settling of the gabion can explain the displacement. The same phenomenon was observed in July 2009 when new gabions were arranged in the upper part of the slope. Also, in this case, a limited portion of the gabion was affected by 2–3 phases of settling that occurred immediately after its construction (Fig. 15a) and without any external trigger; the total displacement was 70 mm in 15 days with a maximum velocity of 19 mm/day.

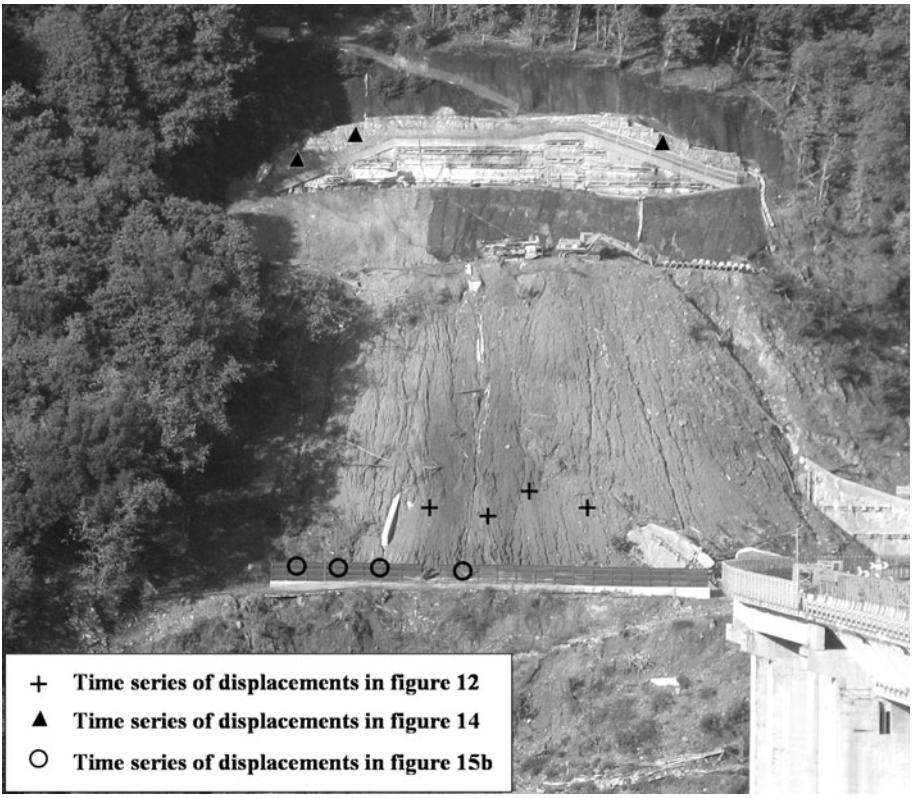

Fig. 11 Location on the slope of the pixels showed in Figs. 12, 14, and 15b

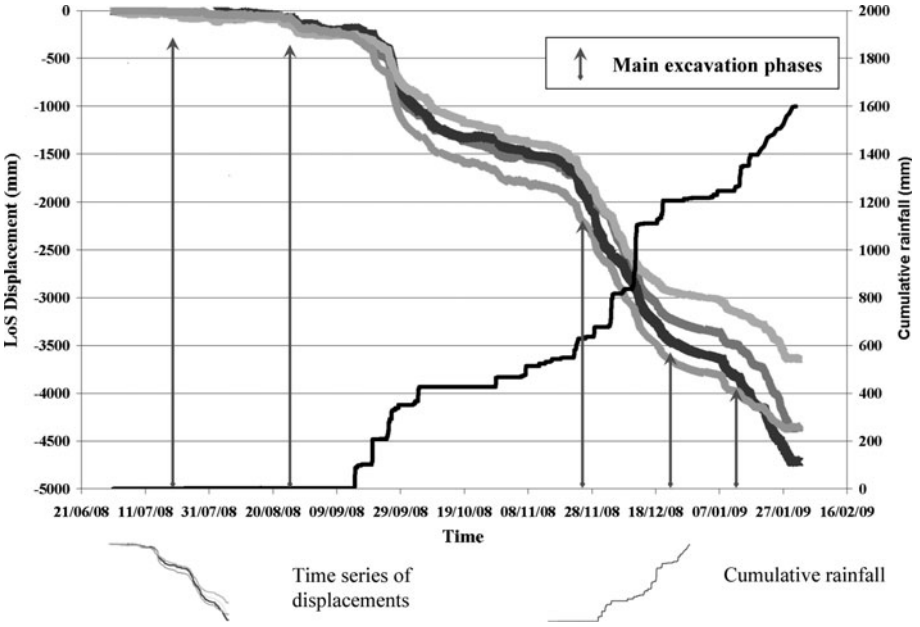

Fig. 12 Cumulative rainfall and displacement time series (June 21, 2008 to January 31, 2009) of some pixels located in the area covered by excavated debris. The *black vertical arrows* identify the main excavation phases

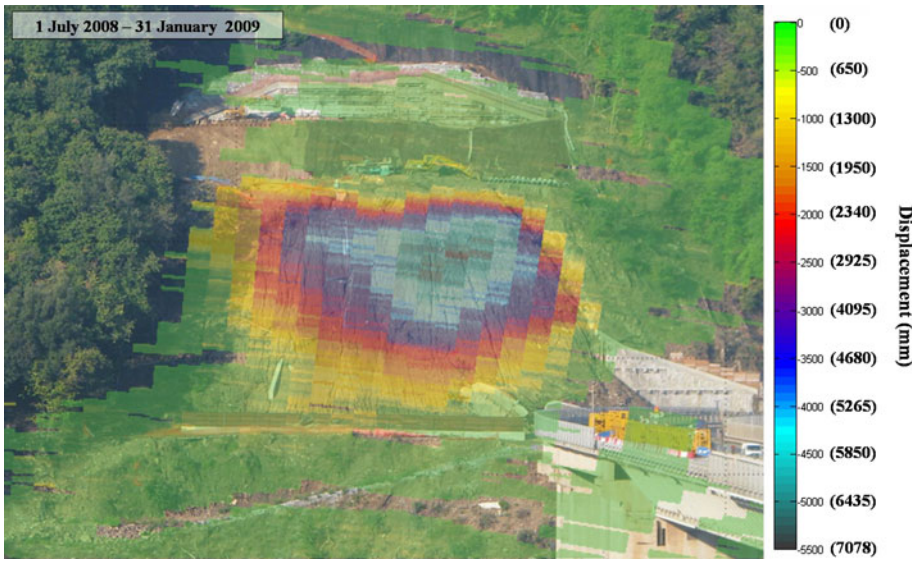

Fig. 13 Picture of the slope overlaid by the cumulative displacement map from July 1, 2008 to January 31, 2009. On the left the LoS displacement, on the right the real displacement of the debris along the slope (modified by Bozzano et al. 2010)

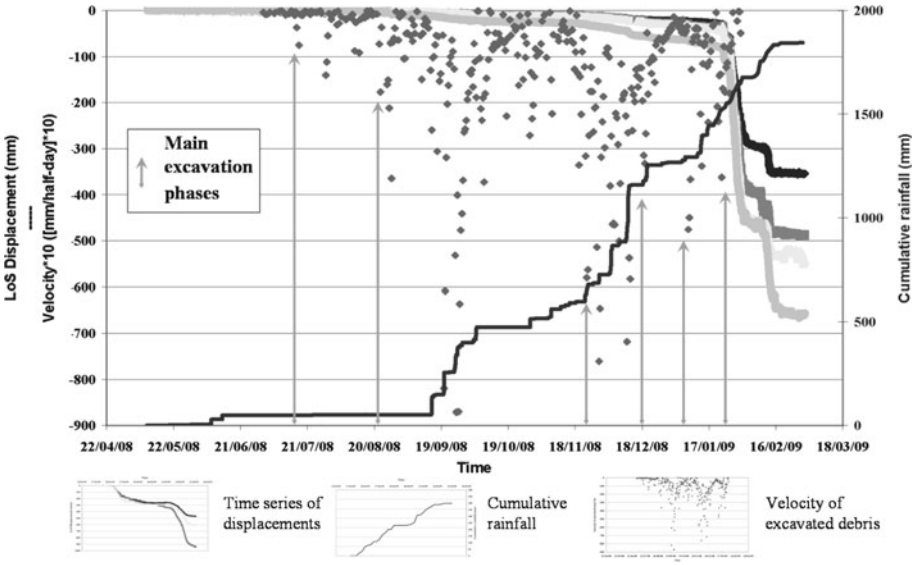

Fig. 14 Cumulative rainfall and displacement time series of some pixels located in the retaining walls and the rate of displacement of the debris (from May, 2008 to February 2009). The *arrows* mark the main excavation phases

Between June 2008 and February 2009, other displacement events were recorded related to extreme rainfall (higher than 100 mm in a few days). In these cases, total displacements between 10 and 40 mm were recorded (Fig. 15b).

4.5 Anchored bulkheads

Anchored bulkheads are among the main structures constructed for slope stabilization. Some tens-of-meters-long anchors were drilled into the old landslide body, thus creating a coupling between the bulkhead and the deeper part of the slope. Three levels of anchored bulkheads were built along the slope from October 2008 to July 2009 (Fig. 4). The expected displacements for such a type of structure are quite limited (some tens of millimeters), and a safety threshold displacement of 40 mm was assumed by the designers. Therefore, millimeter accuracy in the displacement monitoring is required. According to the geological model of the slope, it is reasonable that, after an initial period of adjustment, subsequent displacements recorded for the anchored bulkheads can reflect slope dynamics.

Data acquired from its construction until December 2008 showed the complete stability of the first bulkhead. However, since the middle of December 2008, a movement toward the radar was measured at a nearly constant velocity of about 0.07 mm/day, thus reaching, at the end of September 2009, the total displacement about 23.5 mm (Fig. 16).

Furthermore, due to the high accuracy (<1 mm) in the displacement measurement, it was possible to detect a difference in displacement between the upper and lower part of the bulkhead of about 3–4 mm. Such a gradient in the displacement indicates a tilting mechanism, which is a quite common behavior for bulkheads.

The second bulkhead was built in February 2009, and it started to move immediately after its construction at the same rate as the first one (about 0.07 mm/day). A total

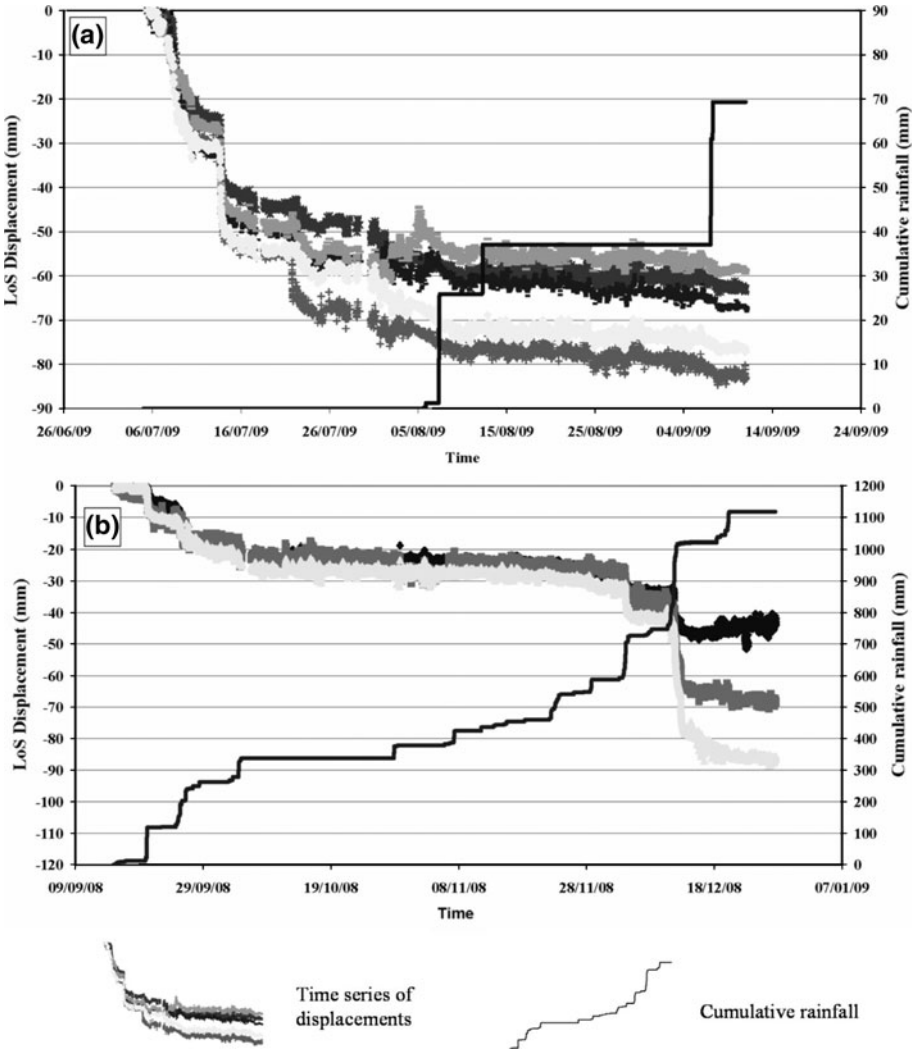

Fig. 15 Cumulative rainfall and displacement time series of some pixels located in the gabions: **a** from July 5, 2009 to September 10, 2009 and **b** from September 15, 2008 to December 27, 2008

displacement of 13 mm was reached at the end of the first 10 days of September 2009 (Fig. 16).

The third bulkhead was finally constructed in June 2009, and similarly to the second, it started to move immediately after its construction at a rate comparable with those of the other bulkheads. A cumulative displacement of 6 mm was reached at the end of the first 10 days of September (Fig. 16).

These displacement values were confirmed by topographic measurements that were periodically performed on some targets over the bulkheads (Fig. 16). However, it must be pointed out that the lower accuracy of these measurements (in the order of 1 cm) allowed to recognize the displacement several months later than interferometric data.

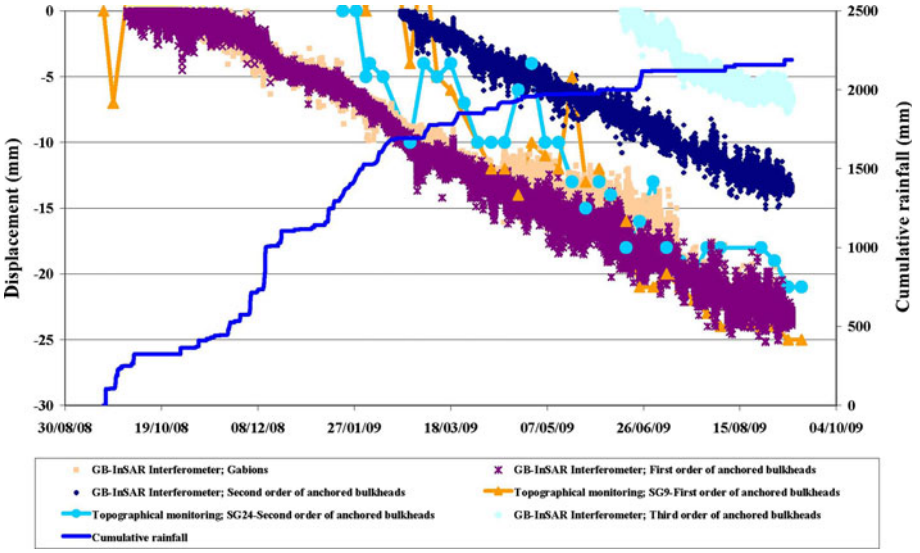

Fig. 16 Displacement time series (obtained by interferometric and topographic monitoring) of the bulkheads from November 2008 to September 2009 and cumulative rainfall

The displacements of these structures were quite regular; hence, it seems to be independent or only slightly influenced by rainfalls.

5 Discussion and conclusions

The remote monitoring platform described in this paper is a prototype for the continuous monitoring of an unstable slope affected by human activities. The completely remote operation allowed continuous monitoring of the slope's evolution and the stability of the man-made structures without any change in instrumental configuration or installation of instruments on the slope. During several phases of the construction activities, the GB-InSAR interferometer was the only instrument able to measure the deformation pattern over the entire slope, thus representing a reference for engineering designers and an important tool to guarantee workers safety. The capability of the technique to monitor slow displacements that occur over long periods as well as rapid movements (up to 1 m/day) allowed the detection of different types of behaviors during the entire monitoring period (23 months). The accuracy of the displacement measurement that ranged from 0.5 to 2 mm (depending on seasonal atmospheric noise) can be considered good enough to monitor each type of expected movement on the slope. As a matter of fact, also the small displacement of the anchored bulkheads was detected in detail.

The large dataset available allowed us to identify different behaviors of the slope and the man-made structures and to correlate them to their triggering factors (Table 2).

It was detected that before the beginning of reconstruction activities, the slope was still affected by shallow instabilities related to residual effects of the landslide that occurred some months before the beginning of the monitoring activity. The main triggering factor for these shallow remobilizations was intense rainfall. Rainfalls were also the most common trigger for other types of shallow surface displacements, such as (1) the sliding of

Table 2 Synoptic table summarizing the main features of displacement pattern

	Total displacement (mm)	Displacement time	Maximum displacement velocity (mm/day)	Maximum displacement acceleration (mm/day^2)	Type of displacement (continuous, intermittent, occasional, etc.)	Usual trigger
Shallow landslides α	250	October 2007–April 2008	25	13	Continuous	Rain
Shallow landslides β	80	October 2007–April 2008	52	35	Occasional	Rain
Shallow landslides γ	550	January 2009–February 2009	77	45.3	Occasional	Rain
Debris produced by excavations	5,500	April 2008–September 2009	190	144	Continuous-intermittent	Human activity, rain
Retaining walls	80	December 2007–February 2009	5.5	4.5	Intermittent	Pushing exerted by upcoming debris
Gabions	85	June 2008–September 2009	19	17	Intermittent	Slope/structure natural interaction, rain
Anchored bulkhead (I order)	23.5	From September 2008	0.1	0.014	Continuous	Slope/structure natural interaction
Anchored bulkhead (II order)	13.3	From February 2009	0.08	0.001	Continuous	Slope/structure natural interaction
Anchored bulkhead (III order)	7	From June 2009	0.41	0.08	Continuous	Slope/structure natural interaction

excavation-derived debris along the slope and (2) the sudden deformations of gabions (occurring when a cumulative value of 100 mm in few days was reached).

Nevertheless, gabions are sometimes displaced also without rainfall or other external triggers. In these cases, the measured displacement is only caused by the gravitational settlement that it is usual for such deformable structure. This peculiar behavior was detected for gabions that were constructed in both June 2008 and July 2009.

Also, in the case of excavated debris, rainfall was not the only triggering or accelerating factor. As a matter of fact, the excavation was a fundamental input for the debris sliding.

Different considerations must instead be made for the anchored bulkheads. First, these structures are anchored in the inner part of the slope; thus, they can also reflect deeper displacements of the slope. Then, they are rigid structures whose deformation must seriously be taken into account when considering the stability of the entire slope. In any case, designers have suggested the displacement value of 40 mm as the prealert threshold for the bulkhead stability. Due to the high accuracy of the ground-based SAR interferometer, we were able to detect initial displacements of less than 1 mm during a couple of weeks in December 2008. Since that time, a total displacement of 25 mm was reached in the first bulkhead. Lower cumulative displacement values were recorded on the other bulkheads (13 and 6 mm, respectively) because they were built later. A similar displacement rate (nearly 0.07 mm/day) was recorded for all the bulkheads. Displacements collected by periodic topographic measurements were quite similar to interferometric ones, thus representing an indirect confirmation of the achieved results. Furthermore, it must be pointed out that the displacement of the bulkheads was almost independent of the rainfall.

Finally, this case history demonstrates that the dataset collected by the integrated platform with a ground-based SAR interferometer may allow to improve the knowledge on the deformational behavior and the related triggering factors of both the natural slope and man-made structures. Furthermore, predictive capabilities for landslide time of collapse have been demonstrated, and further ongoing researches are carrying out in order to achieve a standard for forecasting analyses by GB-InSAR. On the other hand, there are some limitations to GB-InSAR monitoring, such as inoperability in vegetated areas and the masking effect of surface displacements on deeper displacements (which are usually more important for the overall stability of the slope).

However, by combining GB-InSAR data with data collected by topographic and underground inclinometric monitoring, not discussed in this paper, it has been possible to gain a complete understanding of the overall dynamics of the slope; hence, effective remedial counter-measures have been address. Moreover, as it regards the man-made structures, the very detailed information on the displacement behavior (amount, distribution, time requested to work, etc.) obtained by the GB-InSAR monitoring could have interesting engineering outcome.

References

Antonello G, Casagli N, Farina P, Leva D, Nico G, Siebar AJ, Tarchi D (2004) Ground-based SAR interferometry for monitoring mass movements. Landslides 1:21–28

Barla G, Antolini F, Barla M, Mensi E, Piovano G (2010) Monitoring of the Beauregard landslide (Aosta Valley, Italy) using advanced and conventional techniques. Eng Geol 116(3–4):218–235

Blikra LH, Anda E (2006) Åknes/Tafjord prosjektet - Geofagleg samanstilling og oppsummering av undersøkingar og overvaking. NGU Rapport (in Norwegian)

Bozzano F, Mazzanti P, Prestininzi A (2008) A radar platform for continuous monitoring of a landslide interacting with an under-construction infrastructure. Italian J Eng Geol Environ 2:35–50

Bozzano F, Mazzanti P, Prestininzi A, Scarascia Mugnozza G (2010) Research and development of advanced technologies for landslide hazard analysis in Italy. Landslides 7(3):381–385
Brunner FK, Zobl F, Gassner G (2003) On the capability of GPS for landslide monitoring. Felsbau. Rock Soil Eng 21(2):51–54
Capra A, Malara LS, Scicolone B (2004) Analisi delle temperature e delle piogge mensili in Calabria nell'ultimo cinquantennio. Economia montana Linea ecologica 3:31–36
Casagli N, Tibaldi A, Merri A, Del Ventisette C, Apuani T, Guerri L, Fortuny-Guasch J, Tarchi D (2009) Deformation of Stromboli Volcano (Italy) during the 2007 eruption revealed by radar interferometry, numerical modelling and structural geological field data. J Volcanol Geotherm Res 182(3–4):182–200
Casagli N, Catani F, Del Ventisette C, Luzi G (2010) Monitoring, prediction, and early warning using ground-based radar interferometry. Landslides 7(3):291–301
Corsini A, Farina P, Antonello G, Barbieri M, Casagli N, Coren F, Guerri L, Ronchetti F, Sterzai P, Tarchi D (2006) Spaceborne and ground-based SAR interferometry as tools for landslide hazard management in civil protection. Int J Remote Sens 27(12):2351–2369
Curlander JC, McDonough RN (1991) Synthetic aperture radar systems and signal processing. Wiley-Interscience, New York
Fukuzono T (1985) A new method for predicting the failure time of a slope. In: Proceedings of the 4th international conference and field workshop on landslides (Tokyo, 1985), Tokyo University Press, pp 145–150
Guadagno FM, Celico PB, Esposito L, Perriello Zampelli S, Piscopo V, Scarascia-Mugnozza G (1999) The debris flows of 5–6 May 1998 in Campania, Southern Italy. Landslide News 12:5–7
Hanssen RF (2001) Radar interferometry: data interpretation and error analysis. Kluwer, Dordrecht
Iannini L, Monti Guarnieri A, Giudici D (2009) Atmospheric phase screen in ground based radar: statistics and compensation. Fringe 2009 workshop: advances in the science and application of SAR interferometry, 30th November–4th December 2009, Frascati, Rome, Italy
Kraus K, Jansa J, Kager H (1997) Photogrammetry advanced methods and applications, vol 2. Dümmler, Bonn
Martinez-Vazquez A, Fortuny-Guash J (2006) Snow cover monitoring in the swiss alps with a GB-SAR. IEEE Geosci Remote Sens Soc Newsl
Massonet D, Fiegl KL (1998) Radar Interferometry and its application to changes in the earth's surface. Rev Geophys 36(4):441–500
Mazzanti P, Brunetti A, (2010) Assessing rockfall susceptibility by terrestrial SAR interferometry. In: Malet JP, Glade T, Casagli N (eds) Proceedings of the mountain risks international conference, Florence, Italy, 24–26 November 2010, pp 109–114
Muller L (1968) New considerations on the Vajont slide. Int J Rock Mech Min Sci 6:1–91
Noferini L, Pieraccini M, Mecatti D, Luzi G, Atzeni C, Tamburini A, Broccolato M (2005) Permanent scatterers analysis for atmospheric correction in ground-based SAR interferometry. IEEE Trans Geosci Remote Sens 43(7):1459–1471
Noferini L, Pieraccini M, Mecatti D, Macaluso G, Atzeni C, Mantovani M, Marcato G, Pasuto A, Silvano S, Tagliavini F (2007) Using GB-SAR technique to monitor slow moving landslide. Eng Geol 95:88–98
Pieraccini M, Casagli N, Luzi G, Tarchi D, Mecatti D, Noferini L, Atzeni C (2002) Landslide monitoring by ground-based radar interferometry: a field test in Valdarno (Italy). Int J Remote Sens 24(6):1385–1391
Pinna M (1972) La climatologia UTET, Torino, pp 462 (in Italian)
Pipia L, Fabregas X, Aguasca A, Mallorqui J (2006) A comparison of different techniques for atmospheric artefact compensation in GBSAR differential acquisitions. In: Proceedings of IGARSS 2006, pp 3739–3742. doi:10.1109/IGARSS.2006.958
Pugliesi G, Aloisi M, Bonaccorso A, Bonforte A, Cantarero M, Campisi O, Falzone G, Mattia M (2004) The early-warning integrated geodetic system to monitor the Sciara del Fuoco (Stromboli) volcanic landslide. Geophys Res Abstr 6:04276
Sammarco O (2004) A tragic disaster caused by the failure of tailing dams leads to the formation of the Stava 1985. Found Mine Water Environ 23:91–95
Tarchi D, Casagli N, Fanti R, Leva D, Luzi G, Pasuto A, Pieraccini M, Silvano S (2003) Landslide monitoring by using ground-based SAR interferometry: an example of application to the Tessina landslide in Italy. Eng Geol 68:15–30
Teza G, Galgaro A, Zaltron N, Genevois R (2007) Terrestrial laser scanner to detect landslide displacement fields: a new approach. Int J Remote Sens 28(16):3425–3446